PCP
PLANT & CELL PHYSIOLOGY

Accumulation of Cyanobacterial Photosystem II Containing the 'Rogue' D1 Subunit Is Controlled by FtsH Protease and Synthesis of the Standard D1 Protein

Takako Masuda[1,4,†], Martina Bečková[1,†], Zoltán Turóczy[1], Jan Pilný[1], Roman Sobotka[1,2], Joko P. Trinugroho[3], Peter J. Nixon[3], Ondřej Prášil[1,*] and Josef Komenda[1,2,*]

[1]Institute of Microbiology, The Czech Academy of Sciences, Centre Algatech, Opatovický mlýn, Třeboň 37901, Czech Republic
[2]Faculty of Science, University of South Bohemia, Branišovská 1760, České Budějovice 370 05, Czech Republic
[3]Sir Ernst Chain Building-Wolfson Laboratories, Department of Life Sciences, Imperial College London, South Kensington Campus, London SW7 2AZ, UK
[4]Present address: Fisheries Resources Institute, Japan Fisheries Research and Education Agency, Shiogama, Miyagi, 985-0001 Japan.
[†]These authors contributed equally to this work.

*Corresponding authors: Josef Komenda, E-mail, komenda@alga.cz; Ondřej Prášil, E-mail, prasil@alga.cz

(Received 14 July 2022; Accepted 27 March 2023)

Unicellular diazotrophic cyanobacteria contribute significantly to the photosynthetic productivity of the ocean and the fixation of molecular nitrogen, with photosynthesis occurring during the day and nitrogen fixation during the night. In species like *Crocosphaera watsonii* WH8501, the decline in photosynthetic activity in the night is accompanied by the disassembly of oxygen-evolving photosystem II (PSII) complexes. Moreover, in the second half of the night phase, a small amount of rogue D1 (rD1), which is related to the standard form of the D1 subunit found in oxygen-evolving PSII, but of unknown function, accumulates but is quickly degraded at the start of the light phase. We show here that the removal of rD1 is independent of the rD1 transcript level, thylakoid redox state and *trans*-thylakoid pH but requires light and active protein synthesis. We also found that the maximal level of rD1 positively correlates with the maximal level of chlorophyll (Chl) biosynthesis precursors and enzymes, which suggests a possible role for rogue PSII (rPSII) in the activation of Chl biosynthesis just before or upon the onset of light, when new photosystems are synthesized. By studying strains of *Synechocystis* PCC 6803 expressing *Crocosphaera* rD1, we found that the accumulation of rD1 is controlled by the light-dependent synthesis of the standard D1 protein, which triggers the fast FtsH2-dependent degradation of rD1. Affinity purification of FLAG-tagged rD1 unequivocally demonstrated the incorporation of rD1 into a non-oxygen-evolving PSII complex, which we term rPSII. The complex lacks the extrinsic proteins stabilizing the oxygen-evolving Mn_4CaO_5 cluster but contains the Psb27 and Psb28-1 assembly factors.

Keywords: Chlorophyll biosynthesis ● *Crocosphaera watsonii* ● Photosystem II ● Rogue D1 ● *Synechocystis*

Introduction

Cyanobacteria are prokaryotes that perform oxygenic photosynthesis. About half of the known cyanobacterial species also have the genetic capacity to fix nitrogen (Stal and Zehr 2008). Nitrogen fixation, the conversion of atmospheric N_2 to bioavailable ammonium (NH_4^+), is an anaerobic process since the nitrogenase enzyme complex responsible for nitrogen fixation is extremely vulnerable to inactivation by oxygen (Fay 1992, Gallon and Stal 1992). On the other hand, ATP and the reductants (NADPH and reduced ferredoxin) required for nitrogen fixation are mostly produced through the light reactions of oxygenic photosynthesis, which generates molecular oxygen as a by-product of the water oxidation reaction within photosystem II (PSII). Therefore, oxygenic photosynthesis will inhibit nitrogen fixation if performed concurrently in the same cell. One strategy to overcome this problem is to perform nitrogen fixation in specialized cells termed heterocysts (Fay 1992). Another is to separate temporally photosynthetic O_2 evolution and carbon fixation from N_2 fixation. In unicellular diazotrophic cyanobacteria, photosynthesis occurs during the day, while N_2 is fixed during the night (Tuit et al. 2004, Mohr et al. 2010, Dron et al. 2012). However, many aspects of temporal separation have not yet been fully elucidated (Berman-Frank et al. 2003, Zehr 2011).

According to current knowledge, the temporal separation of nitrogen fixation and photosynthesis is accomplished by robust diel metabolic cycles that lead to preferential transcription of photosynthetic genes during the day and nitrogen fixation–related genes during the night (Mohr et al. 2010, Pennebaker et al. 2010, Shi et al. 2010, Dron et al. 2012, Masuda et al. 2018). The diazotroph *Crocosphaera watsonii* WH 8501 has proved to be a useful model to study these cycles (for review, see

Masuda et al. 2022b). When grown under 12-h-light/12-h-dark (12L:12D) cycles, *C. watsonii* cells fix nitrogen during the dark phase (Tuit et al. 2004, Mohr et al. 2010, Dron et al. 2012), while PSII activity peaks in the middle of the light period. Interestingly, a large fraction of PSII is disassembled during the dark phase (Mohr et al. 2010, Pennebaker et al. 2010, Rabouille and Claquin 2016, Masuda et al. 2018) and this appears to be related to a general suppression of membrane protein synthesis (Masuda et al. 2018). Indeed, this especially affects PSII since its key membrane protein D1 exhibits a fast turnover (for review, see Komenda et al. 2012), which can occur even in the dark (Krynická et al. 2015). Intriguingly, a small amount of a paralog of the D1 protein called rogue D1 (rD1, Murray 2012) appears to be incorporated into the PSII monomer during the later stage of the night phase, and this paralog again quickly disappears upon the onset of the light phase (Masuda et al. 2018). The appearance of rD1 in the dark has also been proposed (Wegener et al. 2014) and recently confirmed for *Cyanothece* (Liberton et al. 2022, Masuda et al. 2022a).

The D1 proteins in cyanobacteria have recently been assigned to several groups and subgroups based on their phylogenetic analysis (Sheridan et al. 2020). rD1 is found in many but not all cyanobacteria, and its function remains enigmatic as it lacks the key amino acid residues involved in binding the oxygen-evolving Mn_4CaO_5 cluster and so is unlikely to catalyze water oxidation (Murray 2012, Sheridan et al. 2020). Wegener et al. (2014) have suggested that the rD1 protein in *Cyanothece* is incorporated into PSII complexes to shut down oxygen evolution. However, given the low abundance of rD1 and its occurrence exclusively in the dark, when no oxygen is evolved, such a role seems improbable. Recent data strongly suggested rD1 incorporation into PSII (Masuda et al. 2018), but definitive experimental evidence is still lacking. Another divergent paralog of D1 distinct from rD1 belongs to a group of the so-called super-rogue D1 (srD1) proteins (Murray 2012, Sheridan et al. 2020), which have been unequivocally shown to incorporate into a special type of non-oxygen-evolving super-rogue PSII complex (srPSII) essential for the synthesis of chlorophyll (Chl) *f* (Ho et al. 2016, Trinugroho et al. 2020). *Crocosphaera watsonii*, like many other rD1-containing cyanobacteria, contains the gene for neither srD1 nor Chl *f*.

In the present study, we investigated the environmental factors regulating the accumulation of rD1 during the diel cycle and its role during the dark phase. We also tested whether rD1 was able to assemble into a PSII-like complex. In addition to circadian transcriptional regulation, we found that the standard D1 (sD1) protein, which is incorporated into oxygen-evolving PSII, plays a crucial role in inducing the fast light-dependent rD1 removal by the FtsH2 protease. The positive correlation between the rise in the level of Chl biosynthesis precursors and Chl biosynthesis enzymes and the appearance of rD1 leads us to speculate that rogue PSII (rPSII) might be important for the activation of maximal Chl biosynthesis just before the onset of light when the cell starts to synthesize the photosystems. Importantly, we show that rD1 can assemble into non-oxygen-evolving PSII complexes, lacking the oxygen-evolving enhancer proteins, which we term rPSII complexes.

Diel changes in the expression and accumulation of D1 and rD1 proteins

The genome of *C. watsonii* contains two annotated genes encoding the sD1 protein of PSII and its paralog rD1. To correlate the expression of sD1 with rD1, we monitored transcript levels of the *psbA1* (*CwatDRAFT_1423*) gene encoding sD1 and the *psbA4* (*CwatDRAFT_4668*) gene encoding rD1 using the RT-PCR method during the cultivation of *C. watsonii* cells under 12-h-light/12-h-dark cycles (12L:12D), with irradiance having a sinusoidal time course peaking at 400 μmol photons m^{-2} s^{-1}. The *psbA1* transcript level normalized to the transcript level of the constitutively expressed *rotA* gene (*CwatDRAFT_6490*) increased sharply from the onset of the light period, peaking at around 6 h of the light period (6L), and then decreased from the second half of the light period to the middle of the dark period (6D), before increasing again during the second half of the dark period (**Fig. 1A**, upper panel). In contrast, the transcript level of the *psbA4* gene encoding rD1 showed an opposite temporal pattern as it decreased at the beginning of the light period, reached a minimum at 6L and started to rise again toward the end of the light period and the beginning of the dark period, and then was maintained at this level during the entire dark period (**Fig. 1A**, lower panel).

Using the same light regime, we also monitored the accumulation of sD1 and rD1 proteins by immunoblotting using a purified rD1–specific antibody raised against its unique N-terminus (Masuda et al. 2018). In agreement with the transcriptional data, the level of sD1 increased from the beginning of the light phase, reached a maximum at 6L–9L and then decreased during the dark period (**Fig. 1B**). There was also a noticeable increase in D1 levels at 11D just before the onset of the light phase. On the other hand, the signal of rD1 appeared at 6D, peaked at 11D and disappeared during the early hours of the light phase (**Fig. 1B**). The temporal change of F_v/F_m, an index of photosynthetic activity, followed the temporal change of sD1 at both the gene expression and protein level. Thus, the protein level of sD1, and especially rD1, does not necessarily follow their transcript levels during the diel cycle. This is especially apparent at 11L and 12L time points when there is still a high level of sD1, while its transcript level is reduced and there is no detectable rD1 despite the accumulation of the *psbA4* transcript.

Expression of the *psbA* genes and accumulation of sD1 and rD1 during the extended light and dark phases of the diel cycle

The observed changes in sD1 and rD1 accumulation during the light and dark phases of the diel cycle (**Fig. 1**) were mostly

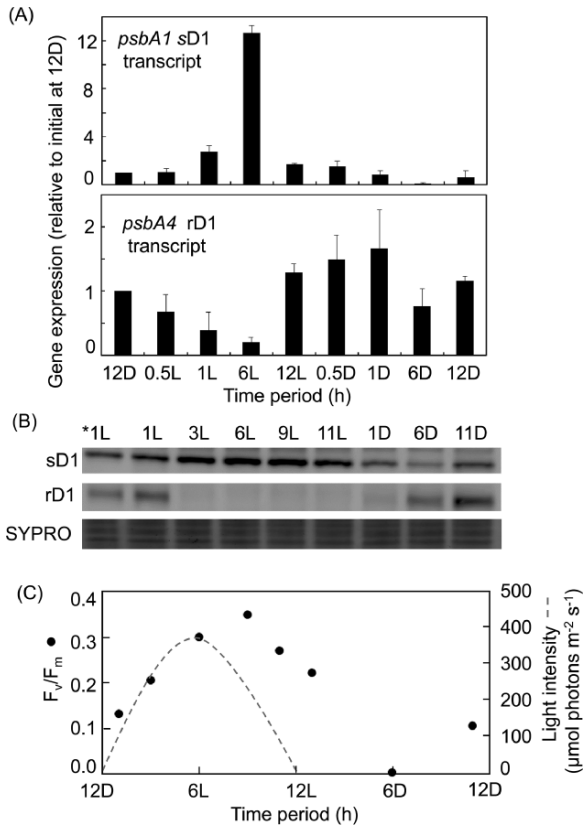

Fig. 1 The temporal changes in *psbA1* and *psbA4* transcript levels (A), accumulation of sD1 and rD1 proteins (B) and changes in PSII activity reflected by the F_v/F_m ratio (C) in *C. watsonii* during the regular 12L:12D diel cycle. (A) The content of sD1 and rD1 transcripts during the diel cycle related to the value of both at 12D (=1). (B) Membranes isolated from cells at a particular time were analyzed by 1D SDS-PAGE, and the gel was stained with SYPRO Orange for general proteins to document equal loading and electroblotted to a polyvinylidene difluoride membrane, which was probed with antibodies specific to sD1 and rD1; each loaded sample contained 2 μg of Chl, and 1L* indicates 50% loading of 1L. (C) The diurnal pattern of the growth irradiance (bell-shaped dotted lines) and values of PSII photochemical yield F_v/F_m (filled circles).

a consequence of circadian-regulated gene transcription, but the observed disconnection of *psbA4* transcription and rD1 accumulation at 11L and 12L time points could be a direct light-driven effect on rD1 synthesis/degradation. To clarify this point, we modified the light regime during the diel cycle. After reaching the maximal irradiance at 6L, either the same light intensity was prolonged for another 24 h or the dark period was extended after 12D for another 24 h. In the first case, the maximal level of the *psbA1* mRNA reached at 6L was strongly suppressed after an additional 12 (18L) or 17 (23L) h of high light, while the *psbA4* transcript levels observed at 18L and 23L were similar to the transcript levels observed at the same time points in the 12L:12D cycles (**Fig. 2A**). This result confirmed the robust transcriptional regulation of both genes by the circadian clock regardless of the light conditions. In line with this regulation, the accumulation of sD1 protein was maximum at 6L, sharply decreased at 18L and partially increased again at 23L, mirroring the level of the *psbA1* transcript (**Fig. 2A, B**) and PSII activity (**Fig. 2C**). Interestingly, the accumulation of rD1 protein mimicked the level of the *psbA4* transcript only in the dark, while no rD1 accumulated despite significant levels of *psbA4* mRNA at 18L and 23L in the light (**Fig. 2A, B**). Apparently, the synthesis and degradation of rD1 are subject to additional post-transcriptional regulation. This was further confirmed in the second case when we extended the dark phase for another 18 h. After an additional 6, 12 and 18 h, the level of rD1 gradually increased, while the sD1 content remained low (**Fig. 3A**). Both sD1 and rD1 were rather stable when chloramphenicol (Cm), an inhibitor of protein synthesis, was added to the cultures during the prolonged dark incubation of 30 h. Thus, in the dark, the synthesis of sD1 is inhibited, while rD1 is still synthesized during the prolonged dark phase despite the fact that the circadian clock–regulated transcript level of sD1 transcript should increase and rD1 transcription should be suppressed based on the true light phase of the cycle.

Testing possible factors controlling the degradation of rD1 in light

The results mentioned earlier suggested that the degradation of rD1 is stimulated by illumination via an unknown post-transcriptional mechanism. To better understand the mechanism, we subjected cells containing rD1 (at 12D) to different light regimes in the presence of various effectors that affect nitrogen availability, protein synthesis, the redox state of the plastoquinone (PQ) pool, the membrane pH gradient and activity of proteases.

We found that the rate of light-dependent disappearance of rD1 is rather independent of light intensity. The decrease in the rD1 level at 1L and 3L was very similar in cells exposed to the standard diel cycle illumination or with light continuously rising from 0 at 12D to 200 μmol photons m^{-2} s^{-1} at 3L or in cells exposed to a constant illumination of 50 μmol photons m^{-2} s^{-1} (**Fig. 4A**). We also tested whether rD1 degradation could be induced just by a short light pulse and then it would continue during the subsequent dark incubation. This would indicate a signaling role of light in the triggering of rD1 degradation. This was assessed by pre-illuminating cells for 5 min before their 3-h dark incubation. Nevertheless, this short light period did not trigger the dark degradation of rD1, which makes light signaling–mediated proteolysis improbable. In addition, we tested whether rD1 degradation could be triggered by the availability of nitrogen, either in the reduced (NH_4^+) form or in the oxidized (NO_3^-) form. None of these compounds changed the rate of rD1 disappearance (**Fig. 4B**).

Illumination has wide-ranging effects on cells including changes to the redox state of the PQ pool and *trans*-thylakoid pH gradient. To judge whether light-induced changes in these characteristics underlie the mechanism of rD1 degradation, we treated cells with specific compounds that influence these characteristics. Light-induced rD1 degradation remained unaffected

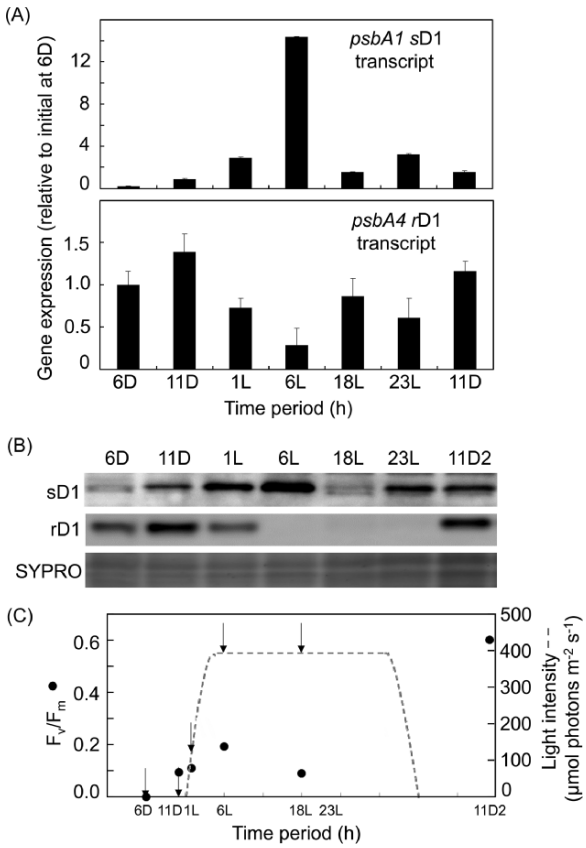

Fig. 2 The temporal changes in *psbA1* and *psbA4* transcript levels (A), accumulation of sD1 and rD1 proteins (B) and changes in PSII activity reflected by the F_v/F_m ratio (C) in *C. watsonii* during the diel cycle with prolonged light exposure. (A) The content of sD1 and rD1 transcripts during the diel cycle related to the value of both at 6D (=1). (B) Membranes isolated from cells at a particular time were analyzed by 1D SDS-PAGE, and the gel was stained with SYPRO Orange for general proteins to document equal loading and electroblotted to a polyvinylidene difluoride membrane, which was probed with antibodies specific to sD1 and rD1. Each loaded sample contained 2 μg of Chl. (C) The diurnal pattern of the growth irradiance (dotted lines) and values of PSII photochemical yield F_v/F_m (filled circles).

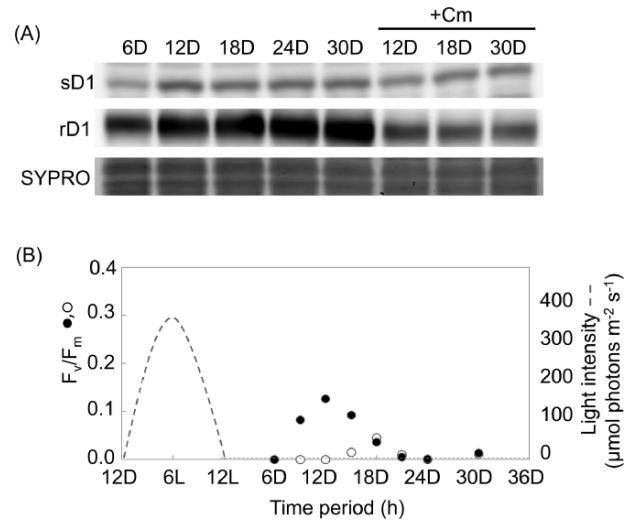

Fig. 3 The temporal changes in the accumulation of sD1 and rD1 proteins (A) and changes in PSII activity reflected by the F_v/F_m ratio (B) in *C. watsonii* during the diel cycle with prolonged dark incubation. (A) Membranes isolated from cells at a particular time were analyzed by 1D SDS-PAGE, and the gel was stained with SYPRO Orange for general proteins to document equal loading and electroblotted to a polyvinylidene difluoride membrane, which was finally probed with antibodies specific to sD1 and rD1. Each loaded sample contained 2 μg of Chl. (B) The diurnal pattern of the growth irradiance (dotted lines) and values of PSII photochemical yield F_v/F_m in cultures non-treated (filled circles) and treated (empty circles) with protein synthesis inhibitor Cm.

in the presence of 2,5-dibromo-6-isopropyl-3-methyl-1,4-benzoquinone (DBMIB), an inhibitor of the cytochrome b_6f complex that causes over-reduction of the PQ pool in the light. Similarly, blocking the PSII activity by 3-(3,4-dichlorophenyl)-1,1-dimethylurea (DCMU) leading to over-oxidation of the PQ pool affected neither rD1 degradation (**Fig. 4C**) nor sD1 and rD1 synthesis (**Supplementary Fig. S1**). When DCMU was combined with oxygen depletion using nitrogen flushing, the rate of rD1 degradation was slightly slowed down in comparison with the control, suggesting some minor inhibitory effect of oxygen removal (**Fig. 4C**). Finally, no apparent difference in the rD1 degradation rate was exerted by the addition of nigericin, an uncoupler of electron transport and *trans*-thylakoid pH gradient, to rD1-containing cells (**Fig. 4D**). In conclusion, light-induced changes to the redox state of PQ or the *trans*-thylakoid pH are not crucial for rD1 degradation.

Although FtsH proteases are considered the main proteases involved in degrading the D1 protein in cyanobacteria (for review, see Komenda et al. 2012), we cannot exclude the possibility that rD1 might be a target for a different cyanobacterial proteolytic system like the Deg serine proteases or Clp (Sokolenko et al. 2002). Therefore, we tested whether the serine protease inhibitor (Pefabloc) can retard rD1 degradation. At 0.5L and 1L, we could see a somewhat higher level of rD1 in Pefabloc-treated cells in comparison with untreated cells (**Fig. 4D**). Thus, some involvement of serine proteases in rD1 removal is possible (see the Discussion section).

Finally, as the illumination of cells could also induce the synthesis of new proteins, for instance proteases, that may be crucial for rD1 degradation, we inhibited protein synthesis during the dark period by adding Cm. Interestingly, at 1L, a similar amount of rD1 to that observed at 12D was detected in the membranes, and this was similar if cells were illuminated by a constant light intensity of 50 μmol photons m^{-2} s^{-1} instead of the standard diel cycle illumination (**Fig. 4E**). The inhibitory effect of Cm was less pronounced at 3L of diel illumination, but rD1 was quite stable even after 3 h of illumination at a constant irradiance of 50 μmol photons m^{-2} s^{-1}. The presence of Cm also stabilized the sD1 protein during the diel illumination. These data suggest the crucial importance of de novo protein synthesis for light-induced rD1 degradation.

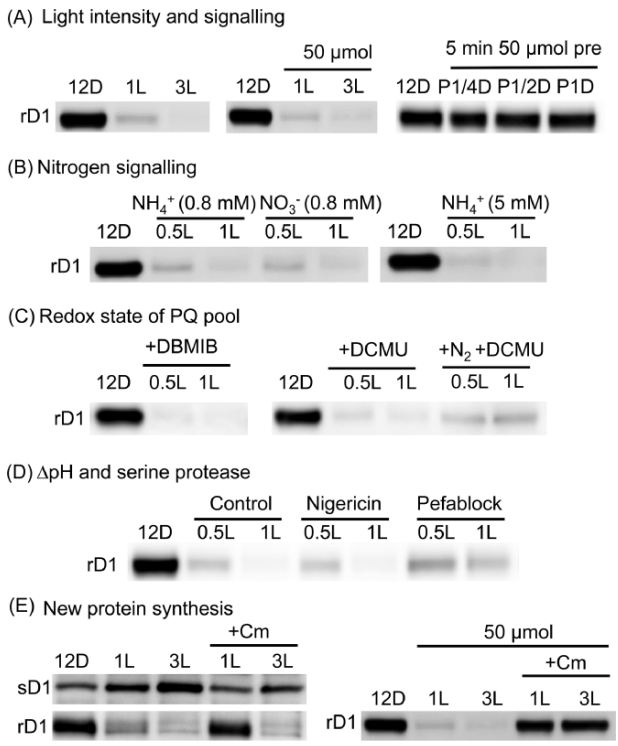

Fig. 4 The temporal changes in the accumulation of sD1 and rD1 protein levels after various treatments affecting light intensity (A), presence of nitrogen (B), redox state of PQ pool (C), *trans*-thylakoid pH and serine protease activity (D) and protein synthesis (E). (A) The content of rD1 was followed after the dark phase of the regular diel cycle and after subsequent 1 and 3 h of constantly increasing diel light intensity (reaching about 200 µmol photons m^{-2} s^{-1} after 3 h; left panel), 3 h of constant illumination of 50 µmol photons m^{-2} s^{-1} (middle panel) or 5-min pre-illumination at 50 µmol photons m^{-2} s^{-1} followed by 1 and 3 h dark incubation (right panel). (B) The content of rD1 was followed after the dark phase of the regular diel cycle and after subsequent 0.5 and 1 h of constantly increasing diel light intensity in the presence of 0.8 and 5 mM NH_4Cl or 0.8 M $NaNO_3$. (C) The content of rD1 was followed after the dark phase of the regular diel cycle and after subsequent 0.5 and 1 h of constantly increasing diel light intensity in the presence of 5 µM DBMIB, 5 µM DCMU and 10 µM DCMU under constant flushing (400 ml min^{-1}) with nitrogen. (D) The content of rD1 was followed after the dark phase of the regular diel cycle and after subsequent 0.5 and 1 h of constantly increasing diel light intensity in the absence and presence of nigericin (50 µM) and serine protease inhibitor Pefabloc SC (500 µM). (E) The content of sD1 and rD1 was followed after the dark phase of the regular diel cycle and after subsequent 1 and 3 h of constantly increasing diel light intensity or constant illumination of 50 µmol photons m^{-2} s^{-1} in the absence and presence of Cm (final concentration: 15 mM). Each loaded sample contained 2 µg of Chl.

Temporal change in biosynthesis and accumulation of Chl during the diel cycle

In our previous study (Masuda et al. 2018), we detected a significant decrease in cellular Chl content during the dark phase of the *C. watsonii* diel cycle. This decrease was verified in the present study (**Supplementary Fig. S2**, white columns). Moreover, we also identified a smaller diameter of the cell in the light phase in comparison with the dark phase (**Supplementary Fig. S2**). In order to see whether the differences in the Chl level during the diel cycle are also accompanied by changes in the level of Chl biosynthesis precursors and enzymes, we assessed their content by HPLC and immunodetection, respectively. The time course of the precursor concentration confirmed the downregulation of Chl biosynthesis during the early stage of the light phase, while it resumed during the dark phase with maximal levels reached at its end (**Fig. 5A**). The only exception was mono-vinyl-chlorophyllide, which decreased during the last 6 h of the dark period in an antiparallel fashion to that of di-vinyl-chlorophyllide. While the former seems to be just partially related to de novo Chl biosynthesis as it partly results from Chl degradation, the latter is clearly a product of de novo Chl biosynthesis (Kopečná et al. 2012). Importantly, the late stages of the dark phase were accompanied by a clear induction of the oxygen-dependent magnesium protoporphyrin IX methylester cyclase (AcsF), which was detected as a double band. We expect that the lower weak band, which was present during the whole diel cycle, is the constitutive 'high-oxygen' AcsF1 cyclase (theoretical calculated mass 40,919 Da). The second band, strongly induced in the dark with a maximum observed at 6D and 11D, is most likely the AcsF2 isozyme (theoreticalcalculated mass 42,493 Da), found in the majority of cyanobacterial species, which is active even under low-oxygen conditions (Chen et al. 2021). Intriguingly, the light-dependent protochlorophyllide oxidoreductase (LPOR) was also strongly induced at 6D and 11D, despite being inactive in the dark, while the light-independent protochlorophyllide reductase (DPOR) version of the enzyme was induced much less. The increased level of AcsF and LPOR at 6D and 11D correlated very well with the appearance of rD1 (**Fig. 5B**). Thus, the presence of rD1 in the cells is limited to the dark period, showing the highest rate of Chl biosynthesis.

Characterization of *Synechocystis* strains expressing rD1 from *C. watsonii*

Firm evidence for the role of rD1 in Chl biosynthesis could be provided by a comparison of the wild-type strain with a mutant strain lacking the *psbA4* gene coding for rD1. However, *C. watsonii* is not easily transformable, and we were not able to obtain the corresponding rD1-less transformant. Therefore, we constructed strains of the naturally transformable cyanobacterium *Synechocystis* sp. PCC 6803 (hereafter *Synechocystis*) that ectopically expresses either the rD1 protein encoded by *C. watsonii* or its N-terminal FLAG-tagged derivative. Instead of using a *Synechocystis* wild-type strain, we used a strain lacking all three *psbA* genes and so unable to synthesize D1 (Debus et al. 1988). The resulting rD1/ΔD1 mutant was unable to grow autotrophically consistent with the inability of rD1 to mediate oxygen evolution. Based on the whole-cell absorption spectrum (**Fig. 6**), the rD1/ΔD1 strain showed a slightly increased cellular level of Chl in comparison with the control D1-less strain, and in the membranes of the strain, we could detect assembled dimeric and monomeric PSII core complexes (termed rPSII,

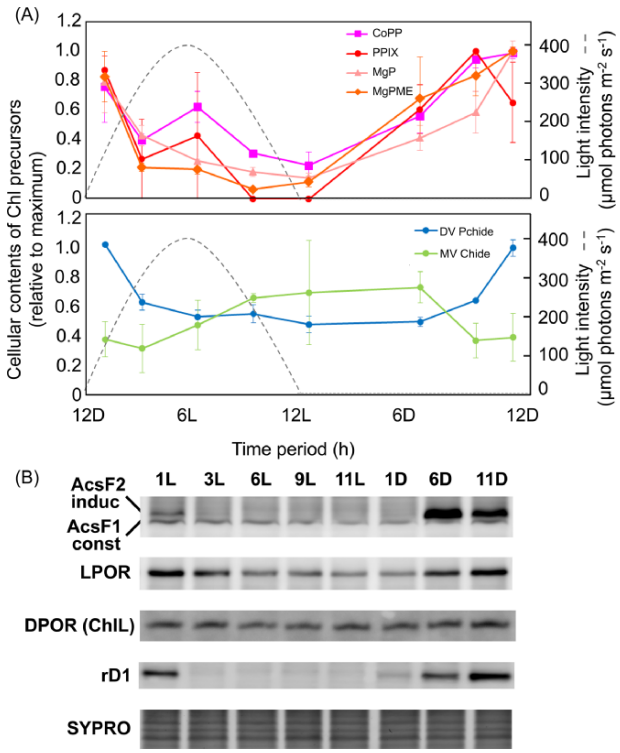

Fig. 5 The cellular content of Chl biosynthesis precursors (A) and Chl biosynthesis enzymes in correlation with rD1 content (B) in *C. watsonii* during the regular 12L:12D diel cycle. (A) The culture of *C. watsonii* was tested during the regular diel cycle for the content of Chl biosynthesis precursors using HPLC analysis. Precursors were quantified as described in the Materials and Methods section. Abbreviations: CoPP, coproporphyrin III; PPIX, protoporphyrin IX; MgP, magnesium protoporphyrin IX; MgPME, magnesium protoporphyrin IX methyl ester; DV Pchlide, di-vinyl-protochlorophyllide; MV Chlide, mono-vinyl-chlorophyllide. (B) The content of Chl biosynthesis enzymes in *C. watsonii* during the regular diel cycle was monitored by 1D SDS-PAGE in combination with immunodetection using the specific antibodies raised against the Chl biosynthesis enzymes and rD1. Each loaded sample contained 0.5 μg of Chl.

Fig. 7). Interestingly, rPSII showed much lower Chl fluorescence than standard PSII (**Fig. 7**, **Supplementary Fig. S3**, 1D fluor), indicating the operation of an effective energy quenching process. We also radiolabeled cells of both strains with [^{35}S]-methionine/cysteine, and after 2D protein gel analysis and autoradiography, we found an increased level of radiolabeled PSI proteins in the rD1-expressing strain in comparison with the control strain (**Fig. 7**). This result is in line with the preferential channeling of newly synthesized Chl molecules into PSI (Kopečná et al. 2012).

Isolation and characterization of PSII complexes containing FLAG-tagged rD1

The expression of the FLAG-tagged version of rD1 in the D1-less *Synechocystis* strain (FLAG-rD1/ΔD1) allowed us to isolate rD1-associated complexes using a FLAG-specific affinity

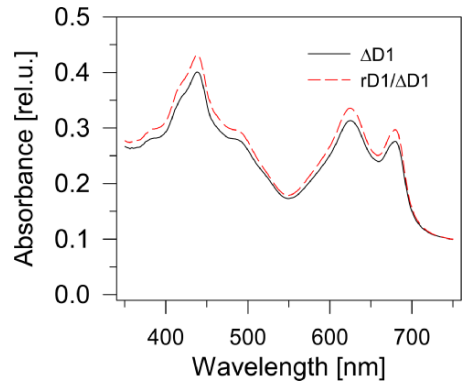

Fig. 6 The whole-cell absorption spectra of *Synechocystis* strains lacking D1 (ΔD1) and lacking D1 but expressing rD1 from *C. watsonii* (rD1/ΔD1). The spectra of cultures adjusted to $OD_{750\ nm} = 0.1$ were measured using the Shimadzu UV-3000.

column. The purified preparation showed an absorption spectrum very similar to that isolated from the D1-less *Synechocystis* strain expressing FLAG-tagged sD1(FLAG-D1/ΔD1; **Fig. 8**, Trinugroho et al. 2020). Its pigment content (32 Chls, nine β-carotenes and two pheophytins per one heme) was also similar to that of FLAG-D1-containing preparation (Trinugroho et al. 2020). Both preparations consisted of PSII core complexes containing FLAG-D1 or FLAG-rD1 and other typical PSII subunits. However, while the FLAG-D1/ΔD1 preparation contained almost equal amounts of PSII dimers and monomers [PSII(2) and PSII(1); **Fig. 9**], the main component of the FLAG-rD1/ΔD1 preparation was a monomer [rPSII(1)] with just a small amount of the dimer [rPSII(2)]. Additionally, we also detected a monomeric PSII complex lacking the CP43 module (rRC47) alone or associated with a monomeric PSI complex [PSI(1)/rRC47]. The preparation lacked the PsbO, PsbV and PsbU extrinsic proteins but contained the Ycf48, Psb27 and Psb28-1 accessory proteins, as identified by mass spectrometry analysis (**Supplementary Table S2**). This analysis also revealed the presence of the PSII auxiliary proteins CyanoP (Knoppová et al. 2016), Psb32 (Wegener et al. 2011) and Psb34 (Zabret et al. 2021, Rahimzadeh-Karvansara et al. 2022), which were not seen in the gel and presumably were present at highly sub-stoichiometric levels.

sD1- and FtsH-dependent degradation of the ectopic rD1 in *Synechocystis* mutants transferred from dark to light

We also constructed and characterized other *Synechocystis* strains with ectopically expressed rD1 to study the mechanism of rD1 degradation in the light. Strain rD1 contains the *psbA4* gene encoding *C. watsonii* rD1 in the *psbA2* locus and expresses the standard *Synechocystis* D1 subunit from the *psbA3* locus. To find out whether rD1 accumulates in this strain just in the dark like in *C. watsonii*, we incubated cells grown in normal light (NL, 40 μmol photons m^{-2} s^{-1}) in the dark for 4 h and then transferred them back to NL for an additional

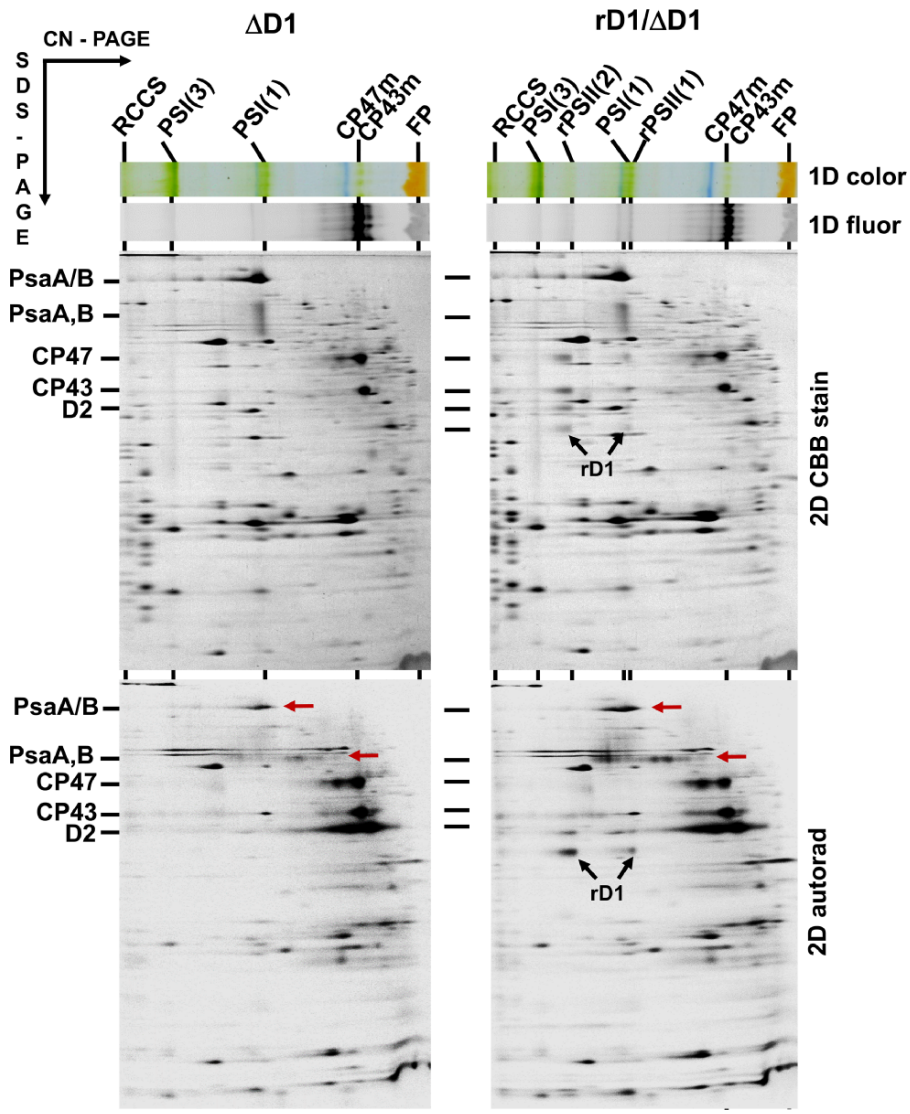

Fig. 7 Analysis of protein accumulation and synthesis in *Synechocystis* strains lacking D1 (ΔD1) and lacking D1 but expressing rD1 from *C. watsonii* (rD1/ΔD1). Membranes from ΔD1 and rD1/ΔD1 cells were analyzed by CN-PAGE in the first dimension. The gel was photographed (1D color) and scanned for Chl fluorescence (1D fluor). After the separation in the second dimension, the 2D gel was stained with Coomassie Blue (2D CBB stain), dried and exposed to a Phosphorimager plate for 24 h (2D autorad). Designations of complexes: RCCS, supercomplex of PSI and PSII; PSI(3), trimeric PSI; rPSII(2), dimeric PSII complex containing rD1; rPSII(1), monomeric PSII complex containing rD1; PSI(1), monomeric PSI complex; CP47m and CP43m, unassembled modules of CP47 and CP47 antennae; FP, free pigments. The horizontal (red) arrows designate the large labeled PsaA/B subunits of PSI. The loading of samples was performed on the same $OD_{750\ nm}$ basis corresponding to 3 μg of Chl of the ΔD1 membranes.

2 h. During this treatment, we sampled the cells and analyzed their membranes by immunoblotting using specific antibodies against sD1 and rD1 (**Fig. 10A**). The results of this analysis confirmed that rD1 in *Synechocystis* behaves in a similar way to native rD1 in *C. watsonii*. There is a gradual appearance in the dark, but after transfer to NL, rD1 quickly disappears. In contrast, the level of sD1 remains stable during the whole treatment. However, when we expressed a FLAG-tagged version of rD1 in the *psbA2* locus, the resulting strain FrD1 (**Fig. 10B**) did not show the light-dependent degradation of FLAG-rD1 and instead its level even slightly increased after transfer from dark to light. These results suggested the possible involvement of the N-terminal tail of rD1 in signaling degradation by the FtsH2/3 protease complex (Komenda et al. 2007). To get stronger experimental evidence for this hypothesis, the gene encoding FtsH2, which has been shown to degrade sD1 in *Synechocystis* (Silva et al. 2003, Komenda et al. 2006), was deleted in the rD1 strain, and the resulting strain (rD1/ΔFtsH2) was subjected to the same treatment as the single rD1 mutant. The stable level of rD1 regardless of the light condition provided strong support for the crucial role of FtsH2 in rD1 degradation (**Fig. 10C**). Finally, to test whether sD1 is

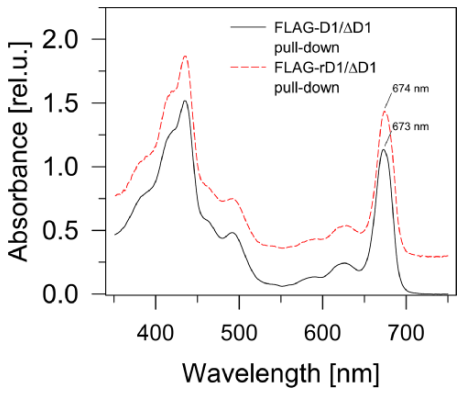

Fig. 8 The absorption spectra of preparations isolated from *Synechocystis* strains lacking D1 but expressing *Synechocystis* FLAG-tagged D1 (FLAG-D1/ΔD1) or *C. watsonii* FLAG-tagged rD1 (FLAG-rD1/ΔD1). The spectra of preparations were measured using the Shimadzu UV-3000 and normalized to the red absorption Chl peak, and the spectrum of the FLAG-rD1/ΔD1 was shifted by 0.25.

needed for the disappearance of rD1 after transfer from dark to light, we also subjected cells of the rD1/ΔD1 strain to a dark–light treatment. The subsequent immunodetection revealed that the level of rD1 was constant regardless of the light conditions, implicating the involvement of light-driven synthesis of sD1 in rD1 degradation (**Fig. 10D**). Interestingly, the absence of sD1 in the rD1/ΔD1 strain led to a large increase of rD1 in comparison with the rD1 levels observed in both the rD1 and rD1/ΔFtsH2 strains (**Supplementary Fig. S4**). In all three strains, sD1 and rD1 were incorporated into PSII complexes as judged by 2D clear-native (CN)/SDS-polyacrylamide gel electrophoresis (PAGE) (**Fig. 7**, **Supplementary Fig. S6**). Overall, the presence of sD1 appears to limit the accumulation of rPSII much more than the degradation of rD1 by FtsH.

Transcriptional and post-transcriptional regulation of sD1 and rD1 proteins in *C. watsonii*

Analysis of *C. watsonii* grown under 12L:12D cycles showed that the transcription of the genes encoding both rD1 and sD1 is primarily driven by a circadian rhythm (**Figs. 1**, **2**). This agrees with previous studies showing circadian gene expression under L/D cycles (Chen et al. 1996, Kucho et al. 2005, Toepel et al. 2008, Zinser et al. 2009, Shi et al. 2010). The cellular level of sD1 corresponded well with its *psbA1* transcript level so that there was an increase in the sD1 content between the second half of the dark period and the middle of the sinusoidal light period, peaking at 400 μmol photons m^{-2} s^{-1}. Conversely, the sD1 level decreased during the second half of the light period and the first half of the dark period (**Fig. 1A–C**) in line with the observed reductions in photosynthetic activity (monitored by light-saturated rates of O_2 evolution), the rate of carbon fixation and F_v/F_m (Masuda et al. 2018, **Figs. 1**, **2**). A major role for circadian transcriptional rhythms in regulating sD1 accumulation was supported by the analysis of cells, grown under the 12L:12D cycle, which had their light period extended from 12 to 24 h. Immunodetection of sD1 showed the loss of sD1 after 18 h of light (**Fig. 2**, 18L), i.e. at midnight in the standard growth regime when the *psbA1* transcript level is at its lowest.

The levels of *psbA4* transcript encoding rD1 went roughly antiparallel with those of sD1, starting to rise at the end of the light phase and increasing further during the dark period. However, the appearance of rD1 did not match the changes in transcript abundance as the protein was detected just in the second half of the night period and quickly disappeared upon the onset of the light period. However, when the light period was extended, rD1 did not appear at the usual time of the diel cycle, despite the rather high level of *psbA4* transcript (**Fig. 2**, 18L and 23L). Conversely, when the dark period was extended, rD1 content slowly increased (**Fig. 3**) despite the circadian clock corresponding to the light phase and low transcript level of rD1 (**Fig. 1**). Thus, the accumulation of rD1 was primarily determined by a post-transcriptional mechanism as its accumulation only occurred in the dark, while in the light the protein was quickly degraded.

What mechanism controls the level of rD1?

As light was apparently the main factor causing the rapid degradation of rD1, we tested various environmental and cellular conditions that could explain the action of light. Our data suggest that light signaling, nitrogen status signaling, the redox state of the PQ pool and *trans*-thylakoid pH (**Fig. 4**) do not play major roles. As only a very limited slowdown of rD1 degradation was observed in the presence of the PSII inhibitor DCMU accompanied by nitrogen flushing, oxygen or its reactive species also do not play a major role in the process. We found that Pefabloc, a serine protease inhibitor, slightly slowed down the light-induced degradation of rD1 (**Fig. 4**), suggesting a possible role for serine proteases in this process although this inhibitor might have some side effects due to its nonspecific binding (Nduaguibe et al. 2010). An even stronger candidate for the rD1 degradation is the FtsH2/FtsH3 protease complex involved in the light-induced degradation of sD1 in cyanobacteria (Silva et al. 2003, Komenda et al. 2006, Nixon et al. 2010). Its involvement was suggested by the inhibition of FLAG-rD1 degradation in a *Synechocystis* strain expressing FLAG-rD1 together with sD1 (**Fig. 10B**). The final convincing evidence for the crucial role of this protease complex was obtained using a *Synechocystis* strain expressing rD1 together with sD1 and lacking FtsH2. Unlike the rD1 strain containing this protease, the rD1/ΔFtsH2 strain was now unable to degrade rD1 upon transfer from dark to light (**Fig. 10C**).

The only treatment we tested that caused a dramatic delay in the light-dependent degradation of rD1 in *C. watsonii* was the inhibition of protein synthesis by Cm. Our evidence that FtsH2/FtsH3 is responsible for light-induced rD1 degradation argues against the involvement of an unknown light-induced/activated protease. Instead, our data support a role for sD1 synthesis in rD1 degradation. First, rD1 expressed in

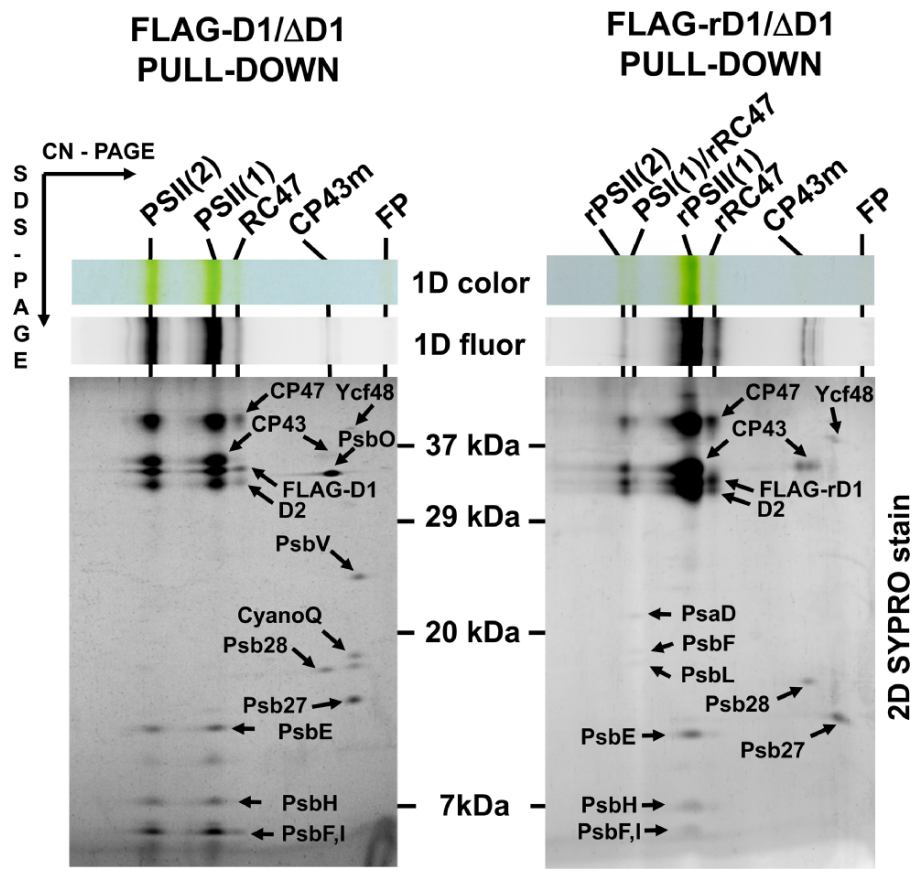

Fig. 9 The analysis of preparations isolated from *Synechocystis* strains lacking D1 but expressing *Synechocystis* FLAG-tagged D1 (FLAG-D1/ΔD1) or *C. watsonii* FLAG-tagged rD1 (FLAG-rD1/ΔD1). Preparations isolated from FLAG-D1/ΔD1 and FLAG-rD1/ΔD1 cells were analyzed by CN-PAGE in the first dimension (1D color). The gel was photographed (1D color) and scanned for Chl fluorescence (1D fluor). After the separation in the second dimension, the 2D gel was stained with SYPRO Orange (2D SYPRO stain). Designations of complexes are as given in **Fig. 7**: PSI(1)/rRC47, the complex of PSI monomer and PSII core lacking CP43 and containing rD1; PSII(2), dimeric PSII complex; PSII(1), monomeric PSII complex; RC47, PSII monomer complex lacking CP43; rRC47, PSII monomer complex lacking CP43 and containing rD1. Each loaded sample contained 0.5 μg of Chl.

the rD1/ΔD1 strain was not degraded after the transfer of cells from dark to light. Second, in the strain rD1, expressing both rD1 and sD1, rD1 accumulates, but after transfer to light, when the level of the *psbA3* transcript encoding sD1 increases and sD1 is intensively synthesized (**Supplementary Fig. S5**), rapid degradation of rD1 is induced. The degradation of rD1 appears to be immediately followed by co-translational incorporation of newly synthesized sD1 into PSII complexes as we were unable to detect either rD1 or sD1 in an unassembled state, even in the absence of FtsH2 (**Supplementary Fig. S6**).

The mechanistic explanation of how newly synthesized D1 triggers the degradation of 'assembled' D1 is unclear. The synthesis of D1 and its incorporation into PSII during assembly occurs in biogenesis centers (Nixon et al. 2010), where precursor PSII complexes with newly inserted D1 might be protected from protease action by auxiliary protein factors like CyanoP, prohibitins and others (Knoppová et al. 2016, 2022). In our view, the most probable explanation for the synchronization of D1 synthesis and degradation is that the intensive synthesis of D1 expels previously assembled/repaired complexes into regions of the membrane where PSII is no longer protected from protease action and might be degraded by the FtsH2/FtsH3 complex. A possible location of rPSII in biogenesis centers would agree with the presence of the Psb27 and Psb28-1 accessory factors in the complex. Given the crucial importance of the N-terminus of D1 for its degradation (Komenda et al. 2007), the N-terminus of rD1, which is markedly different from that of sD1, may trigger rD1 degradation preferentially in comparison with sD1. However, we cannot exclude the possible post-translational modification of rD1 in selective replacement as rD1 migrates as a double band in SDS-PAGE gels, with the upper part retained after transfer from dark to light in the FtsH2-less strain (**Fig. 10C**).

The overall regulation of sD1 and rD1 synthesis and accumulation is akin to the regulation of expression of the low light (D1:1) and high light (D1:2) forms of D1 in *Synechococcus* sp. PCC 7942, which occurs at both the transcriptional and translational levels (Tyystjärvi et al. 2001, 2004). After shifting

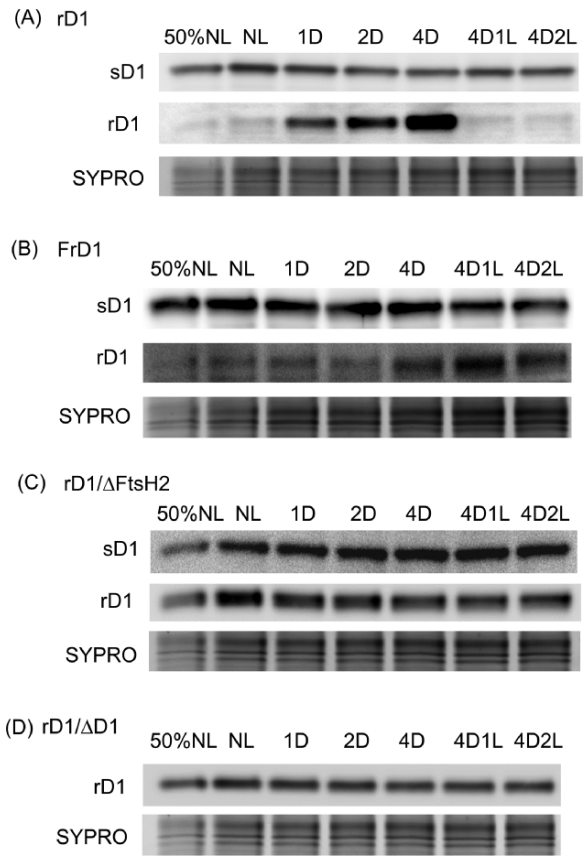

Fig. 10 The temporal changes in the accumulation of sD1 and rD1 proteins in *Synechocystis* strains (A) containing the original D1 and expressing rD1 from *Crocosphaera* (rD1), (B) containing the original D1 and expressing FLAG-tagged rD1 (FrD1), (C) containing the original D1, expressing rD1 from *Crocosphaera* and lacking FtsH2 (rD1/ΔFtsH2) and (D) lacking the original D1 and expressing rD1 from *Crocosphaera* (rD1/ΔD1). The content of sD1 and rD1 in cells of all four strains grown in the presence of 5 mM Glc was followed in control cells (NL), cells incubated in the dark for 1, 2 and 4 h (1D, 2D and 4D) and after subsequent transfer from dark to light for 1 and 2 h (4D1L and 4D2L). Cells were used for the isolation of membranes, which were analyzed by SDS-PAGE. The gel was stained with SYPRO Orange to document equal loading and transblotted to PVDF membrane, and sD1 and rD1 were detected by specific antibodies. Each loaded sample contained 1 μg of Chl, samples designated 50% NL contained just 0.5 μg of Chl.

Synechococcus cells from high to low light, D1:2 is rapidly degraded and replaced by D1:1. Given that the inhibition of protein synthesis practically blocks D1:2 degradation after transferring to low light (Komenda et al. 1999), it has been speculated that newly synthesized D1:1 induces the degradation of D1:2. Interestingly, even the degradation of radioactively labeled sD1 in *Synechocystis* is accelerated by the presence of newly synthesized sD1 (Komenda and Barber 1995, Komenda et al. 2000), which would indicate that synchronization between the synthesis and degradation of D1 is a universal feature of the D1 degradation process.

The function of rD1 in cyanobacteria

The physiological role of rD1 in various cyanobacteria has not yet been satisfactorily explained. In the present study, we obtained the first unequivocal evidence for the incorporation of rD1 into non-oxygen-evolving PSII complexes (rPSII). A possible role for rPSII in suppressing PSII oxygen evolution during periods of low light to allow the nitrogenase to function more rapidly is an attractive idea (Wegener et al. 2014) but does not seem probable, given that the level of rPSII is quite low and nitrogenase acts during the dark phase when no oxygen can be evolved and when there is ongoing active respiration. Moreover, the time course of nitrogenase activity does not match the kinetics of the appearance of rD1 (Masuda et al. 2018).

Instead, we obtained several circumstantial pieces of experimental evidence to suggest a role for rPSII in Chl biosynthesis in the dark. First, there was a good correlation between the nocturnal appearance of rD1, the increase in the Chl level and the steady-state levels of Chl precursors and enzymes of the Chl biosynthesis pathway (especially AcsF and LPOR). The vast majority of Chl in *C. watsonii* is associated with PSI (Masuda et al. 2018), and its increase should therefore be especially reflected in the higher abundance of PSI. In agreement with this, the transcriptional analysis of *C. watsonii* during the diel cycle (Shi et al. 2010) showed increasing transcript abundance of the PsaA/PsaB Chl-binding proteins of PSI as well as the PSI assembly factors Ycf3, Ycf4 and Ycf37 during the later stages of the dark phase (see also **Supplementary Table S3**). For this period of the diel cycle, the enhanced transcription of several Chl biosynthesis enzymes and PSII assembly factors like Psb27 and Psb28 was also observed. Particularly, the parallel nocturnal upregulation of AcsF and Psb28-1 supports a relationship between both proteins as revealed from the study of a Psb28-1-less strain of *Synechocystis* (Dobáková et al. 2009). In contrast, the main structural proteins of PSII, with the exception of rD1, did not show such an enhanced transcription (**Supplementary Table S3**), which would suggest that the assembly of rPSII involves the recycling of PSII subunits originating from the disassembly of sD1-containing PSII complexes. Indeed, the requirement of both PSII activity and assembled PSII complexes alone for maximal rates of Chl biosynthesis and for the accumulation of PSI (the main sink for Chl) has also been shown in *Synechocystis* (Kiss et al. 2019). Chl biosynthesis in cyanobacteria occurs mostly in the light using the LPOR enzyme (Kopečná et al. 2013). However, this enzymatic step is also functional in the dark, thanks to the presence of the DPOR enzyme (Fujita and Bauer 2003), a widespread nitrogenase-like enzyme assumed to be sensitive to oxygen (Yamazaki et al. 2006). Interestingly, LPOR appears even more accumulated in the second half of the dark phase than DPOR (**Fig. 5**). A possible explanation is that cells prepare for the light phase to immediately start light-dependent Chl biosynthesis and/or LPOR plays a structural or regulatory role in the activity of DPOR and low-oxygen cyclase enzyme formed by the AcsF2 catalytic subunit and the Ycf54 factor (Chen et al. 2021). One possibility is that AcsF2 together with

protochlorophyllide reductases may be stabilized in the dark by interacting with rPSII or rRC47 with bound Psb27 or Psb28-1, respectively. Nevertheless, we were not able to detect any of these enzymes in the isolated rPSII, which could be caused by their weak or transient interaction with the complex. Previously, AcsF was only detected in RC47 isolated using His-tagged Psb28-1, which might stabilize this interaction (Dobáková et al. 2009). The ability of rPSII to efficiently quench Chl fluorescence (**Fig. 8**, **Supplementary Fig. S3**) may also suggest a possible role of rPSII in the photoprotection of biogenesis centers upon the sudden appearance of light, such as at sunrise.

The role of rD1 in Chl biosynthesis is also supported by the analysis of a D1-less *Synechocystis* strain expressing *C. watsonii* FLAG-rD1. It is notable that in the rD1/ΔD1 strain, the synthesis and accumulation of PSI increased in comparison with the control D1-less strain (**Figs. 6**, **7**) although both strains could not evolve oxygen and grew photoheterotrophically. The FLAG-rD1 pull-down contained mostly monomeric FLAG-rPSII lacking oxygen-evolving enhancer proteins but was associated with PSII assembly factors Psb27, Psb28 and other auxiliary proteins. Interestingly, among them, there was also a hypothetical protein Slr1917, which contains the α/β hydrolase fold (Interpro IPR000073) and might represent a *Synechocystis* homolog of plant Chl dephytylases involved in Chl turnover (Lin et al. 2022). This type of enzyme (a homologous gene encoding this enzyme in *C. watsonii* is CwatDRAFT_0930) might be involved in the redistribution of newly synthesized Chl between various Chl-binding proteins as such redistribution may require phytyl detachment/reattachment (Vavilin et al. 2005). The FLAG-rD1/ΔD1 eluate also contained a small amount of a complex between a PSI monomer and rRC47. We speculate that this complex might be a PSI synthesis intermediate incorporating new Chl molecules with the assistance of rRC47. Although the involvement of rPSII in Chl biosynthesis is still hypothetical, it is tempting to speculate that rPSII and the related srPSII complex (Ho et al. 2016, Trinugroho et al. 2020) might participate in Chl biosynthesis through formation, stabilization and photoprotection of a Chl biosynthesis metabolon.

Cultivation of *C. watsonii*, experimental conditions and monitoring of growth

Stock cultures of *C. watsonii* WH 8501 were obtained from the Culture Collection Yerseke (the Royal Netherlands Institute for Sea Research, Netherlands, Yerseke, the strain number CCY 0601). Cells were maintained in an N-free YBC-II medium (Chen et al. 1996) at 28°C in glass flasks under the constant white light of 150 μmol photons m^{-2} s^{-1} using a 12L:12D cycle. Diluting them every ∼12 d kept cell densities within 200,000–6,000,000 cells ml^{-1}. At the beginning of each experiment, cultures were transferred into flat panel photobioreactors (FMT150, Photon System Instruments, Brno, the Czech Republic) (Nedbal et al. 2008), with a sinusoidal 12L:12D growth irradiance peaking at 400 μmol photons m^{-2} s^{-1}. Cultures were acclimated to these conditions and maintained exponential growth for at least five generations (∼10 d). The photobioreactors continuously recorded F_o and F_t (every 5 min) as well as F_m and F_m' (every 30 min), which were then used to calculate in situ diurnal changes in F_t and F_m by averaging datasets of seven consecutive days. Cell abundance was measured by a cell counter (Beckman, Multisizer 4, Brea, CA, USA). To determine Chl concentration, we collected 10 ml of culture by centrifugation (8,000 rpm × 8 min) and measured Chl absorbance in methanol extract (Porra et al. 1989)

Synechocystis strains and growth conditions

All *Synechocystis* strains used in the study were based on the glucose-tolerant wild-type substrain called GT-P (Tichý et al. 2016). The pPD-*N*FLAG vector was used to express the *C. watsonii* rD1 from the *psbA2* locus of *Synechocystis*, either in its native D1 form or with an N-terminal 3xFLAG-tag (Hollingshead et al. 2016). The rD1-encoding *psbA4* gene from *C. watsonii* was amplified using a Phusion High-Fidelity PCR Master Mix (New England Biolabs, Ipswich, MA, USA) with genomic DNA as a template and a specific set of primers (**Supplementary Table S1**). Plasmids were constructed by In-Fusion cloning (Zhu et al. 2007). The resulting plasmids, designated pPD-rD1 and pPD-FLAG-rD1, were used to transform the D1-less triple *psbA* deletion strains (ΔD1; Trinugroho et al. 2020) to yield rD1/ΔD1 and FLAG-rD1/ΔD1 mutants. The strain FLAG-D1/ΔD1 expressing the FLAG-tagged native form of the *Synechocystis* D1 was constructed in a similar way using specific primers (**Supplementary Table S1**) as described by Trinugroho et al. (2020).

To generate rD1 and FLAG-rD1 mutant strains in *Synechocystis*, we transformed cells of *Synechocystis* GT-P strain (Tichý et al. 2016) with genomic DNA isolated from rD1/ΔD1 and FLAG-rD1/ΔD1 strains, respectively, where *psbA4* and *FLAG-psbA4* genes are placed under the *psbA2* promoter and carrying kanamycin-resistance cassettes. Cells were then segregated on plates with BG11 medium and kanamycin, and segregation of cells was verified with PCR using primers located up- and downstream of the *psbA2* gene (psbA2f 3′-TGTCAT CTATAAGCTTCGTG-5′ and psbA2re 3′-ATCCGCCGGCAGACGTTCTTCC-5′, **Supplementary Fig. S7A**). To generate mutant strains rD1/ΔFtsH2 and FLAG-rD1/ΔFtsH2 in *Synechocystis*, we transformed newly generated rD1 and FLAG-rD1 mutant strains with genomic DNA isolated from ΔFtsH2 strains with erythromycin (Mann et al. 2000, Komenda et al. 2006) and Cm-resistance cassettes inserted into the *ftsH2* (*slr0228*) gene (Komenda et al. 2010), respectively. The full segregation was verified with PCR using primers located in the *ftsH2* (*slr0228*) gene (slr0228F 3′-AGAACTGCCCTACTTTGG-5′ and slr0228re 3′-GATAGCGGATTTACGACG-5′, **Supplementary Fig. S7B**) and with primers psbA2f and psbA2re to verify the background segregation (**Supplementary Fig. S7A**).

Synechocystis strains were cultivated on glucose BG-11 agar plates [BG-11 basic mineral medium, supplemented with 0.3% (w/v) sodium thiosulfate, 10 mM TES-KOH pH = 8.2, 5 mM glucose and 1.5% (w/v) agar]. Fifty milliliters of liquid BG-11 cultures containing 5 mM glucose (and appropriate antibiotics when necessary) were grown in 250-ml sterile Erlenmeyer flasks on an orbital shaker at approximately 100 rpm. The strains were incubated in a temperature-controlled room set at 27–29°C and illuminated with a fluorescent white light of intensity 35 μmol photons m^{-2} s^{-1}. For the isolation of FLAG-rD1-containing complexes, 4 l of the FLAG-rD1/ΔD1 mutant cells were grown in a 10-l air-bubbled flask under 35 μmol photons m^{-2} s^{-1}.

Determination of the maximum quantum yield of PSII

Chl fluorescence parameter F_v/F_m representing the maximum quantum yield of PSII was measured using a portable AquaPen-C AP-C100 fluorometer (Photon Systems Instruments, Brno, the Czech Republic) in 2-ml aliquots withdrawn from the bioreactor as described by Masuda et al. (2018).

RNA isolation, reverse transcription and quantitative PCR

For RNA extraction, 20 ml of *C. watsonii* culture was collected and centrifuged, and the pellet was resuspended in the PGTX buffer (Pinto et al. 2009) and frozen

in liquid nitrogen for RNA isolation. For RNA isolation, cells in the PGTX buffer were incubated at 95°C for 5 min, RNA was extracted with chloroform and finally, RNA was precipitated by isopropanol. After washing with 75% ethanol, the precipitate was air-dried and dissolved in RNase-free water. For the cDNA synthesis, 2 μg of the total RNA was DNase-treated by using the TURBO DNA-free Kit (Thermo Fisher Scientific, Waltham, MA, USA), and the Transcriptor First-Strand cDNA Synthesis Kit (Roche Life Science, Mannheim, Germany) was used for cDNA synthesis using gene-specific reverse primers (**Supplementary Table S1**). Real-time quantitative PCR reactions were performed on the Rotor-Gene 3000 using the iQ SYBR Green Supermix (Bio-Rad, Hercules, CA, USA). Primer sets for the *psbA4* gene (*CwatDRAFT_4668*) coding for rD1, the *psbA1* gene (*CwatDRAFT_1423*) coding for sD1 and the constitutively expressed *rotA* (*CwatDRAFT_6490*), encoding a peptidyl-prolyl *cis-trans* isomerase (Dyhrman and Haley 2011) used for normalization, are described in **Supplementary Table S1**. The same procedure was applied for the quantification of *psbA4* and *psbA3* transcripts in *Synechocystis* strains expressing *psbA4* from the *psbA2* promotor, except for the reverse transcription reaction where random hexamers were used. Primer sets used for the quantification of the *psbA4* gene (*CwatDRAFT_4668*) coding for rD1, the *psbA3* gene (*sll1867*) coding for sD1 and *rnpB* (encoding the B subunit of ribonuclease P) as a reference gene (Krynická et al. 2014) are described in **Supplementary Table S1**. All analyses were performed in triplicates, and the obtained data were analyzed by relative quantification using the $2^{-\Delta\Delta Ct}$ method (Livak and Schmittgen 2001).

Radioactive labeling of cells

Radioactive pulse labeling of the cells was performed at 500 μmol photons m^{-2} s^{-1} and 30°C using a mixture of [^{35}S]Met and [^{35}S]Cys (Hartmann Analytic GmbH, Braunschweig, Germany) as described previously (Masuda et al. 2018).

Isolation of membranes and protein analyses

Cyanobacterial membrane proteins were isolated by breaking cells with glass beads and solubilizing membrane proteins in 1% *n*-dodecyl-β-D-maltoside to analyze their proteins by CN-PAGE (Komenda et al. 2012). Samples of equal Chl content (3 μg) were loaded onto the gel. The protein composition of the complexes was analyzed by electrophoresis in a denaturing 16–20% linear gradient polyacrylamide gel containing 7 M urea. Gels with separated proteins were stained with Coomassie Blue. For autoradiography, the membrane with labeled proteins was exposed to a Phosphorimager plate (GE Healthcare, Uppsala, Sweden) overnight. The standard one-dimensional analysis of proteins was performed on the same 16–20% linear gradient polyacrylamide gel containing 7 M urea, which was stained with SYPRO Orange and then transferred onto a polyvinylidene difluoride membrane. Membrane proteins were incubated with specific primary antibodies against functional D1 present in cyanobacteria (Boehm et al. 2012), N-terminus of the *C. watsonii* rD1 (Masuda et al. 2018), LPOR enzyme (Kopečná et al. 2012), L-subunit of the DPOR from *Leptolyngbia* (Yamazaki et al. 2006) and plant CHL27 homolog of AcsF (Tottey et al. 2003) and then with secondary antibody–horseradish peroxidase conjugate (Sigma-Aldrich, St. Louis, MO, USA).

Isolation of the rD1-containing complexes

Large-scale membrane preparations for the purification of proteins and their complexes were isolated using Mini-Beadbeater-16, the membranes were solubilized with *n*-dodecyl-β-D-maltoside and FLAG-tagged proteins were isolated using the anti-FLAG M2 affinity gel (Sigma-Aldrich) as described in detail by Koskela et al. (2020).

Whole-cell absorption spectroscopy and pigment determination

Absorption spectra of whole cells were measured at room temperature using a UV-3000 spectrophotometer (Shimadzu, Kyoto, Japan) and were measured in the cultures with the identical optical density at 750 nm ($OD_{750\,nm}$). For routine Chl determination, pigments were extracted from cell pellets with 100% methanol, and the Chl concentration was determined spectroscopically (Porra et al. 1989). For detailed analysis of Chl biosynthesis precursors, they were extracted by an excess of 70% methanol from 2 ml of cell cultures. Their detection was performed by an Agilent 1200 HPLC instrument (Agilent Technologies, Santa Clara, CA, USA). The fluorescence detector FLD1 was set to the excitation/emission maxima of 440/660 nm to detect the Chl precursors monovinyl-chlorophyllide, di-vinyl-chlorophyllide and di-vinyl-protochlorophyllide, while coproporphyrin III and protoporphyrin IX were detected at 400/620 and 400/630 nm, respectively. Mg-protophorphyrin IX and Mg-protophorphyrin IX monomethyl ester were detected using the fluorescence detector FLD2 set to an excitation/emission maxima of 416/595 nm (Pilný et al. 2015).

Supplementary data are available at *PCP* online.

The data underlying this article are available in the article and in its online supplementary material.

The Czech Science Foundation (20-17627S to T.M. and O.P., 19-29225X to M.B., J.P., R.S. and J.K.); the Biotechnology and Biological Sciences Research Council (BB/P00931X/1 to P.J.N.); the award of a PhD Scholarship from the Indonesia Endowment Fund for Education (to J.P.T.).

We are grateful for excellent technical support by Jana Zahradníková.

O.P. and J.K. designed the research. T.M., M.B., Z.T., J.P., R.S. and J.K. performed the experiments. T.M., M.B., Z.T., J.P., R.S. and J.K. analyzed the data. J.K. wrote the draft. All authors contributed to the final manuscript writing.

The authors have no conflicts of interest to declare.

Berman-Frank, I., Lundgren, P. and Falkowski, P. (2003) Nitrogen fixation and photosynthetic oxygen evolution in cyanobacteria. *Res. Microbiol.* 19: 162–173.

Boehm, M., Jianfeng, Y., Krynická, V., Barker, M., Tichý, M., Komenda, J., et al. (2012) Subunit organization of a *Synechocystis* hetero-oligomeric thylakoid FtsH complex involved in photosystem II repair. *Plant Cell* 24: 3669–3683.

Debus, R.J., Barry, B.A., Sithole, I., Babcock, G.T. and McIntosh, L. (1988) Directed mutagenesis indicates that the donor to P680+ in photosystem II is tyrosine-161 of the D1 polypeptide. *Biochemistry* 27: 9071–9074.

Dobáková, M., Sobotka, R., Tichý, M. and Komenda, J. (2009) The Psb28 protein is involved in the biogenesis of the photosystem II inner antenna CP47 (PsbB) in the cyanobacterium *Synechocystis* sp. PCC 6803. *Plant Physiol.* 149: 1076–1086.

Dron, A., Rabouille, S., Claquin, P., Le Roy, B., Talec, A. and Sciandra, A. (2012) Light-dark (12:12) cycle of carbon and nitrogen metabolism in *Crocosphaera watsonii* WH8501: relation to the cell cycle. *Environ. Microbiol.* 14: 967–981.

Dyhrman, S.T. and Haley, S.T. (2011) Arsenate resistance in the unicellular marine diazotroph *Crocosphaera watsonii*. *Front. Microbiol.* 2: 214.

Fay, P. (1992) Oxygen relations of nitrogen-fixation in cyanobacteria. *Microbiol. Rev.* 56: 340–373.

Fujita, Y. and Bauer, C.E. (2003) The light-independent protochlorophyllide reductase: a nitrogenase-like enzyme catalyzing a key reaction for greening in the dark. *In* Porphyrin Handbook, Vol. 13, Chlorophylls and Bilins: Biosynthesis, Synthesis, and Degradation. Edited by Kadish, K.M., Smith, K.M. and Guilard, R. pp. 109–156. Academic Press, San Diego, CA.

Gallon, J.R. and Stal, L.J. (1992) N_2 fixation in nonheterocystous cyanobacteria—an overview. *In* Marine Pelagic Cyanobacteria: *Trichodesmium* and Other Diazotrophs. Edited by Carpenter, E.J., Capone, D.G. and Rueter, J.G. pp. 115–139. Kluwer Academic Publishers, Dordrecht.

Hollingshead, S., Kopečná, J., Armstrong, D.R., Bučinská, L., Jackson, P.J., Chen, G.E., et al. (2016) Synthesis of chlorophyll-binding proteins in a fully segregated Δ*ycf54* strain of the cyanobacterium *Synechocystis* PCC 6803. *Front. Plant. Sci.* 7: 292.

Ho, M.Y., Shen, G.Z., Canniffe, D.P., Zhao, C. and Bryant, D.A. (2016) Light-dependent chlorophyll f synthase is a highly divergent paralog of PsbA of photosystem II. *Science* 353: aaf9178.

Chen, G.E., Hitchcock, A., Mareš, J., Gong, Y., Tichý, M., Pilný, J., et al. (2021) Evolution of Ycf54-independent chlorophyll biosynthesis in cyanobacteria. *Proc. Natl. Acad. Sci. U.S.A.* 118: e2024633118.

Chen, Y.B., Zehr, J.P. and Mellon, M. (1996) Growth and nitrogen fixation of the diazotrophic filamentous nonheterocystous cyanobacterium *Trichodesmium* sp IMS 101 in defined media: evidence for a circadian rhythm. *J. Phycol.* 32: 916–923.

Kiss, É., Knoppová, J., Pascual Aznar, G., Pilný, J., Yu, J., Halada, P., et al. (2019) Photosynthesis-specific rubredoxin-like protein is required for efficient association of the D1 and D2 proteins during the initial steps of photosystem II assembly. *Plant Cell* 31: 2241–2258.

Knoppová, J., Sobotka, R., Yu, J., Bečková, M., Pilný, J., Trinugroho, J.P., et al. (2022) Assembly of D1/D2 reaction center complexes of photosystem II: stepwise binding of pigments and a network of auxiliary proteins. *Plant Physiol.* 189: 790–804.

Knoppová, J., Yu, J., Koník, P., Nixon, P.J. and Komenda, J. (2016) CyanoP is involved in the early steps of photosystem II assembly in the cyanobacterium *Synechocystis* sp. PCC 6803. *Plant Cell Physiol.* 57: 1–11.

Komenda, J. and Barber, J. (1995) Comparison of psbO and psbH deletion mutants of *Synechocystis* PCC 6803 indicates that degradation of D1 protein is regulated by the QB site and dependent on protein synthesis. *Biochemistry* 34: 9625–9631.

Komenda, J., Barker, M., Kuviková, S., de Vries, R., Mullineaux, C.W., Tichý, M., et al. (2006) The FtsH protease Slr0228 is important for quality control of photosystem II in the thylakoid membrane of *Synechocystis* sp PCC 6803. *J. Biol. Chem.* 281: 1145–1151.

Komenda, J., Hassan, H.A.G., Diner, B.A., Debus, R.J., Barber, J. and Nixon, P.J. (2000) Degradation of the photosystem II D1 and D2 proteins in different strains of the cyanobacterium *Synechocystis* PCC 6803 varying with respect to the type and level of psbA transcript. *Plant Mol. Biol.* 42: 635–645.

Komenda, J., Knoppová, J., Kopečná, J., Sobotka, R., Halada, P., Yu, J.F., et al. (2012) The Psb27 assembly factor binds to the CP43 complex of photosystem II in the cyanobacterium *Synechocystis* sp PCC 6803. *Plant Physiol.* 158: 476–486.

Komenda, J., Knoppová, J., Krynická, V., Nixon, P.J. and Tichý, M. (2010) Role of FtsH2 in the repair of photosystem II in mutants of the cyanobacterium *Synechocystis* PCC 6803 with impaired assembly or stability of the CaMn4 cluster. *Biochim. Biophys. Acta* 1797: 566–575.

Komenda, J., Koblížek, M. and Masojídek, J. (1999) The regulatory role of photosystem II photoinactivation and de novo protein synthesis in the degradation and exchange of two forms of the D1 protein in the cyanobacterium *Synechococcus* PCC 7942. *J. Photochem. Photobiol.* 48: 114–119.

Komenda, J., Tichý, M., Prášil, O., Knoppová, J., Kuviková, S., de Vries, R., et al. (2007) The exposed N-terminal tail of the D1 subunit is required for rapid D1 degradation during photosystem II repair in *Synechocystis* PCC 6803. *Plant Cell* 19: 2839–2854.

Kopečná, J., Komenda, J., Bučinská, J. and Sobotka, R. (2012) Acclimation of the cyanobacterium *Synechocystis* 6803 to high light is accompanied by an enhanced production of chlorophyll that is preferentially channeled to trimeric PSI. *Plant Physiol.* 160: 2239–2250.

Kopečná, J., Sobotka, R. and Komenda, J. (2013) Inhibition of chlorophyll biosynthesis at the protochlorophyllide reduction step results in the parallel depletion of photosystem I and photosystem II in the cyanobacterium *Synechocystis* PCC 6803. *Planta* 237: 497–508.

Koskela, M.M., Skotnicová, P., Kiss, É. and Sobotka, R. (2020) Purification of protein-complexes from the cyanobacterium *Synechocystis* sp. PCC 6803 using FLAG-affinity chromatography. *Bio. Protoc.* 10: e3616.

Krynická, V., Shao, S., Nixon, P.J. and Komenda, J. (2015) Accessibility controls selective degradation of photosystem II subunits by FtsH protease. *Nat. Plants* 1: 15168.

Krynická, V., Tichý, M., Krafl, J., Yu, J., Kaňa, R., Boehm, M., et al. (2014) Two essential FtsH proteases control the level of the Fur repressor during iron deficiency in the cyanobacterium *Synechocystis* sp. PCC 6803. *Mol. Microbiol.* 94: 609–624.

Kucho, K., Okamoto, K., Tsuchiya, Y., Nomura, S., Nango, M., Kanehisa, M., et al. (2005) Global analysis of circadian expression in the cyanobacterium *Synechocystis* sp. strain PCC 6803. *J. Bacteriol.* 187: 2190–2199.

Liberton, M., Biswas, S. and Pakrasi, H.B. (2022) Photosynthetic modulation during the diurnal cycle in a unicellular diazotrophic cyanobacterium grown under nitrogen-replete and nitrogen-fixing conditions. *Sci. Rep.* 12: 18939.

Lin, Y.P., Shen, Y.Y., Shiu, Y.B., Charng, Y.Y. and Grimm, B. (2022) Chlorophyll dephytylase 1 and chlorophyll synthase: a chlorophyll salvage pathway for the turnover of photosystems I and II. *Plant J.* 111: 979–994.

Livak, K.J. and Schmittgen, T.D. (2001) Analysis of relative gene expression data using real-time quantitative PCR and the 2(-Delta Delta C(T)) method. *Methods* 25: 402–408.

Mann, N.H., Novac, N., Mullineaux, C.W., Newman, J., Bailey, S. and Robinson, C. (2000) Involvement of an FtsH homologue in the assembly of functional photosystem I in the cyanobacterium *Synechocystis* sp PCC 6803. *FEBS Lett.* 479: 72–77.

Masuda, T., Bernát, G., Bečková, M., Kotabová, E., Lawrenz, E., Lukeš, M., et al. (2018) Diel regulation of photosynthetic activity in the oceanic unicellular diazotrophic cyanobacterium *Crocosphaera watsonii* WH8501. *Environ. Microbiol.* 20: 546–560.

Masuda, T., Inomura, K., Gao, M., Armin, G., Kotabová, E., Bernát, G., et al. (2022a) The balance between photosynthesis and respiration explains the niche differentiation between *Crocosphaera* and *Cyanothece*. *Comp. Struct. Biotech. J.* 21: 58–65.

Masuda, T., Inomura, K., Mareš, J. and Prášil, O. (2022b) *Crocosphaera watsonii*. *Trends Microbiol.* 30: 805–806.

Mohr, W., Intermaggio, M.P. and LaRoche, J. (2010) Diel rhythm of nitrogen and carbon metabolism in the unicellular, diazotrophic cyanobacterium *Crocosphaera watsonii* WH8501. *Environ. Microbiol.* 12: 412–421.

Murray, J.W. (2012) Sequence variation at the oxygen evolving centre of photosystem II: a new class of 'rogue' cyanobacterial D1 proteins. *Photosyn. Res.* 110: 177–184.

Nduaguibe, C.C., Bentsi-Barnes, K., Mullen, Y., Kandeel, F. and Al-Abdullah, I. (2010) Serine protease inhibitors suppress pancreatic endogenous proteases and modulate bacterial neutral proteases. *Islets* 2: 200–206.

Nedbal, L., Trtílek, M., Červený, J., Komárek, O. and Pakrasi, H.B. (2008) A photobioreactor system for precision cultivation of photoautotrophic microorganisms and for high-content analysis of suspension dynamics. *Biotechnol. Bioeng.* 100: 902–910.

Nixon, P.J., Michoux, F., Yu, J., Boehm, M. and Komenda, J. (2010) Recent advances in understanding the assembly and repair of photosystem II. *Ann. Bot.* 106: 1–16.

Pennebaker, K., Mackey, K.R.M., Smith, R.M., Williams, S.B. and Zehr, J.P. (2010) Diel cycling of DNA staining and nifH gene regulation in the unicellular cyanobacterium *Crocosphaera watsonii* strain WH 8501 (Cyanophyta). *Environ. Microbiol.* 12: 1001–1010.

Pilný, J., Kopečná, J., Noda, J. and Sobotka, R. (2015) Detection and quantification of heme and chlorophyll precursors using a high performance liquid chromatography (HPLC) system equipped with two fluorescence detectors. *Bio. Protoc.* 5: e1390.

Pinto, F.L., Thapper, A., Sontheim, W. and Lindblad, P. (2009) Analysis of current and alternative phenol based RNA extraction methodologies for cyanobacteria. *BMC Mol. Biol.* 10: 79.

Porra, R.J., Thompson, W.A. and Kriedemann, P.E. (1989) Determination of accurate extinction coefficients and simultaneous equations for assaying chlorophylls *a* and *b* extracted with four different solvents: verification of the concentration of chlorophyll standards by atomic absorption spectroscopy. *Biochim. Biophys. Acta* 975: 384–394.

Rabouille, S. and Claquin, P. (2016) Photosystem-II shutdown evolved with nitrogen fixation in the unicellular diazotroph *Crocosphaera watsonii*. *Environ. Microbiol.* 18: 477–485.

Rahimzadeh-Karvansara, P., Pascual-Aznar, G., Bečková, M. and Komenda, J. (2022) Psb34 protein modulates binding of high-light-inducible proteins to CP47-containing photosystem II assembly intermediates in the cyanobacterium *Synechocystis* sp. PCC 6803. *Photosynth. Res.* 152: 333–346.

Sheridan, K.J., Duncan, E.J., Eaton-Rye, J.J. and Summerfield, T.C. (2020) The diversity and distribution of D1 proteins in cyanobacteria. *Photosynth. Res.* 145: 111–128.

Shi, T., Ilikchyan, I., Rabouille, S. and Zehr, J.P. (2010) Genome-wide analysis of diel gene expression in the unicellular N_2-fixing cyanobacterium *Crocosphaera watsonii* WH 8501. *ISME J.* 4: 621–632.

Silva, P., Thompson, E., Bailey, S., Kruse, O., Mullineaux, C.W., Robinson, C., et al. (2003) FtsH is involved in the early stages of repair of photosystem II in *Synechocystis* sp PCC 6803. *Plant Cell* 15: 2152–2164.

Sokolenko, A., Pojidaeva, E., Zinchenko, V., Panichkin, V., Glaser, V.M., Herrmann, R.G., et al. (2002) The gene complement for proteolysis in the cyanobacterium *Synechocystis sp.* PCC 6803 and *Arabidopsis thaliana* chloroplasts. *Curr. Genet.* 41: 291–310.

Stal, L.J. and Zehr, J.P. (2008) Cyanobacterial nitrogen fixation in the ocean: diversity, regulation, and ecology. *In* The Cyanobacteria: Molecular Biology, Genomics and Evolution. Edited by Herrero, A. and Flores, E. pp. 423–446. Caister Academic Press, Norfolk.

Tichý, M., Bečková, M., Kopečná, J., Noda, J., Sobotka, R. and Komenda, J. (2016) Strain of *Synechocystis* PCC 6803 with aberrant assembly of photosystem II contains duplication of a large part of the genomic DNA. *Front. Plant Sci.* 7: 648.

Toepel, J., Welsh, E., Summerfield, T.C., Pakrasi, H. and Sherman, L.A. (2008) Differential transcriptional analysis of the cyanobacterium *Cyanothece* sp. strain ATCC 51142 during light-dark and continuous-light growth. *J. Bacteriol.* 190: 3904–3913.

Tottey, S., Block, M.A., Allen, M., Westergren, T., Albrieux, C., Scheller, H.V., et al. (2003) Arabidopsis CHL27, located in both envelope and thylakoid membranes, is required for the synthesis of protochlorophyllide. *Proc. Natl. Acad. Sci. U.S.A.* 100: 16119–16124.

Trinugroho, J.P., Bečková, M., Shao, S., Yu, J., Zhao, Z., Murray, J.W., et al. (2020) Chlorophyll *f* synthesis by a super-roque photosystem II complex. *Nat. Plants* 6: 238–244.

Tuit, C., Waterbury, J. and Ravizza, G. (2004) Diel variation of molybdenum and iron in marine diazotrophic cyanobacteria. *Limnol. Oceanogr.* 49: 978–990.

Tyystjärvi, T., Herranen, M. and Aro, E.M. (2001) Regulation of translation elongation in cyanobacteria: membrane targeting of the ribosome nascent-chain complexes controls the synthesis of D1 protein. *Mol. Microbiol.* 40: 476–484.

Tyystjärvi, T., Sirpiö, S. and Aro, E.M. (2004) Post-transcriptional regulation of the *psbA* gene family in the cyanobacterium *Synechococcus* sp. PCC 7942. *FEBS Lett.* 576: 211–215.

Vavilin, D., Brune, D.C. and Vermaas, W.F.J. (2005) ^{15}N-labeling to determine chlorophyll synthesis and degradation in *Synechocystis* sp. PCC 6803 strains lacking one or both photosystems. *Biochim. Biophys. Acta* 1708: 91–101.

Wegener, K.M., Bennewitz, S., Oelmüller, R. and Pakrasi, H.B. (2011) The Psb32 protein aids in repairing photodamaged photosystem II in the cyanobacterium *Synechocystis* 6803. *Mol. Plant* 4: 1052–1061.

Wegener, K.M., Nagarajan, A. and Pakrasi, H.B. (2014) An atypical *psbA* gene encodes a sentinel D1 protein to form a physiologically relevant inactive photosystem II complex in cyanobacteria. *J. Biol. Chem.* 290: 3764–3774.

Yamazaki, S., Nomata, J. and Fujita, Y. (2006) Differential operation of dual protochlorophyllide reductases for chlorophyll biosynthesis in response to environmental oxygen levels in the cyanobacterium *Leptolyngbya boryana*. *Plant Physiol.* 142: 911–922.

Zabret, S., Bohn, S.K., Schuller, O., Arnolds, O., Möller, M., Meier-Credo, J., et al. (2021) Structural insights into photosystem II assembly. *Nat. Plants* 7: 524–538.

Zehr, J.P. (2011) Nitrogen fixation by marine cyanobacteria. *Trends Microbiol.* 19: 162–173.

Zhu, B., Cai, G., Hall, E.O. and Freeman, G.J. (2007) In-FusionTM assembly: seamless engineering of multidomain fusion proteins, modular vectors, and mutations. *Biotechniques* 43: 354–359.

Zinser, E.R., Lindell, D., Johnson, Z.I., Futschik, M.E., Steglich, C., Coleman, M.L., et al. (2009) Choreography of the transcriptome, photophysiology, and cell cycle of a minimal photoautotroph, *Prochlorococcus*. *PLoS One* 4: e5135.